ELSEVIER

Journal of Nuclear Materials 283–287 (2000) 1116–1120

journal of nuclear materials

www.elsevier.nl/locate/jnucmat

Development of functionally graded plasma-facing materials

Chang-Chun Ge [a,*], Jiang-Tao Li [a], Zhang-Jian Zhou [a], Wen-Bin Cao [a], Wei-Ping Shen [a], Ming-Xu Wang [b], Nian-Man Zhang [b], Xiang Liu [b], Zheng-Yu Xu [b]

[a] *Laboratory of Special Ceramics and Powder Metallurgy, University of Science and Technology Beijing, Beijing 100083, People's Republic of China*

[b] *Southwest Institute of Nuclear Physics, Chengdu 610041, People's Republic of China*

Abstract

Three different processing technologies are described for the fabrication of SiC/C functionally graded material (FGM), B_4C/Cu coating FGM and W/Cu FGM. The microstructure and physical properties of the FGMs are evaluated. Some plasma-relevant performances of these three FGMs show their prospect as plasma-facing materials in fusion reactors.

1. Introduction

Graphite is widely used in present Tokamak facilities and a C/C composite has been selected as one of the candidate materials for the ITER. But C-based material has excessive chemical sputtering yield at 600–1000 K and exhibits irradiation-enhanced sublimation at >1200 K under plasma erosion conditions, causing serious C-contamination of plasma. Hence, various measures are being taken to solve this problem. Introducing Si- and B-containing organic compounds and He through in situ glow discharge in Tokamak facilities results in Si- and B-based films which can effectively reduce the contamination of light impurities in plasma, but the thickness is limited to a range of 70–100 nm. However, the life time is too short, and this kind of film is ineffective for high heat flux components (such as divertor etc.) as the film will rapidly erode [1–5].

Low Z materials SiC and B_4C have several advantages for use in fusion reactors, such as excellent high temperature properties, corrosion resistance, low density and, especially for SiC, low activation after irradiation [6]. To reduce C contamination during plasma exposure, SiC or B_4C coatings have been deposited on the surface of C substrates with various processes [7–9]; however, thermal stresses arise on the interface between the coating layer and the substrate under high temperature heating/cooling cycles from the difference in thermal expansion coefficients, leading to cracks or peeling in the SiC or B_4C coating.

Tungsten has the highest sputtering threshold of all possible candidates, with a high melting point; it will be the first candidate in highly loaded plasma-interactive components of commercial fusion reactors. But joining W to Cu heat sinks has a series of difficulties, one of which is the mismatch of thermal expansion coefficients between the two materials ($\alpha_W = 4\times10^{-6}/°C$, $\alpha_{Cu} = 18\times10^{-6}/°C$). This causes large thermal stress during fabrication and service and leads to cracks on the interface between W and Cu [2,10].

Japanese scientists first proposed the idea of functionally graded materials (FGMs) in 1984. Inhomogeneous materials with gradually varying compositions and structures were made in order to reduce thermal stresses and, thus, cracks and failure [11,12].

In previous studies, SiC/C composites and FGM were fabricated with CVD or CVI process, but this process cycle was long (in some cases 100 h), the cost was high and it was difficult to obtain thick graded layers [11]. Many FGM systems have been made with a powder stacking–hot pressing process, but hot-pressed SiC/C FGM is rare. W/Cu FGMs have been made with

* Corresponding author.
E-mail address: gehome@public3.bta.net.cn (C.-C. Ge).

0022-3115/00/$ - see front matter
PII: S0022-3115(00)00318-4

various powder metallurgical processes, but a B_4C/Cu coated FGM has not yet been reported.

On the basis of our previous studies on FGM [12,13], in this paper, the FGM design idea is applied to three kinds of composites – SiC/C, B_4C/Cu and W/Cu – to combine the advantages of the high thermal shock resistance and thermal conductivity of graphite and copper with the high plasma erosion resistance of SiC, B_4C and W for use as plasma-facing materials (PFM). Three different processing technologies are correspondingly used for these three kinds of FGM and some primary results of plasma-relevant characteristics of these materials are reported.

2. Fabrication and evaluation procedures

2.1. SiC/C FGM

At first, specimens of monolithic SiC and C and SiC/C composites with 100% SiC, 75% SiC + 25% C, 50% SiC + 50% C, 25% SiC + 75% C, 100% C and 2-layered SiC/C were hot pressed. For monolithic SiC, Al–B–C was used as sintering aid. Sintering was done at 1800°C, 1850°C, 1900°C and 1950°C, with a pressure of 20 MPa for 1 h. For 2-layered SiC/C and SiC/C composites, the sintering was done at 1900°C for 1 h at 20 MPa. Five-layered SiC/C FGM 20 mm in diameter × 5 mm thick were fabricated under the same conditions. Table 1 lists the density of the SiC/C composites with different compositions. The density is calculated, taking the theoretical density of graphite to be $\rho = 1.89$ g/cm^3. The morphology and bonding interface between layers were observed with scanning electron microscope. The bonding between various layers of the SiC/C FGM specimen was good. Each layer was closely bonded with its neighboring layers.

Many properties of graphite, such as thermal conductivity, electrical conductivity, thermal shock resistance, etc., depend on the degree of graphitization (DG), which is determined from spell-out patterns of the specimens. The SiC/C composites had higher DG than high-strength graphite ($DG_{graphite} = 50$–60%), and the DG increased with the C content of the composite. This characteristic is a good basis for making SiC/C FGM with favorable thermal conductivity, electrical conductivity and thermal shock resistance.

Thermal shock resistance was measured on 2-layered specimens and SiC/C FGM specimens, which were repeatedly heated to 900°C, kept at 900°C for 2 min in an $MoSi_2$ furnace and quenched in water at room temperature. For 2-layered SiC/C specimens, cracks and peeling occurred after five times, while no cracking or peeling appeared in SiC/C FGM after 20 repetitions.

2.2. B_4C/Cu FGM

Commercial B_4C powder with a particle size of 20 μm and Cu powder with a particle size of −200 mesh were used as coating materials. They were sprayed on Cu substrates with dimensions of 10 mm × 10 mm × 2 mm, 10 mm × 20 mm × 2 mm and 15 mm diameter × 2 mm thickness. Before coating with B_4C, an Ni–Al alloy was applied to the substrates. Argon was used for the plasma gas, while hydrogen was usually added to enhance the gas–particle heat transfer to aid particle melting and to suppress oxygen contamination in the coated layer. To make a B_4C/Cu non-FGM coating, B_4C powder was sprayed on the substrate without any transition layer. The thickness of B_4C coating layer varied from 160 to 260 μm. To make B_4C/Cu FGM coatings, B_4C/Cu coating FGM with different composition distribution exponents ($P = 0.2$, 1.0, 2.0) were fabricated with this process, where P is determined from the equation: $VF = (x/d)^P$, in which VF expresses the volume fraction of Cu in certain layer of the FGM, x is the distance of this layer with the surface layer and d is the thickness of the coating FGM. The specimens were repeatedly heated in an $MoSi_2$ furnace to 500°C and kept for 5 min, then quenched in water. It is found that coating FGM with $P = 1.0$ had much better hot shock resistance than with $P = 0.2$ and 2.0. No peeling appeared after 20 cycles for specimens with $P = 1.0$, while peeling happened after 2–5 cycles for specimens with $P = 0.2$ and 2.0.

C1 and C2 are used to denote specimens of B_4C/Cu non-FGM coating with thickness of 160 and 260 μm. C3 and C4 are used to denote B_4C/Cu FGM coating with thickness of 160 and 260 μm and $P = 1.0$.

2.3. W/Cu FGM

Several W/Cu FGMs were fabricated. In the first case, W powder with particle sizes of 3, 7 and 15 μm with 99.9% purity and 40 μm Cu powder with 99% purity were used. W powders with different particle sizes (with 3 μm for the first layer, 7 μm for the second layer and 15 μm for the third layer) were mixed

Table 1
Densities and relative densities of SiC/C composites with different compositions

	100% SiC	75% SiC + 25% C	50% SiC + 50% C	25% SiC + 75% C	100% C
ρ	3.12	2.82	2.50	2.19	1.87
ρ/ρ_{th}	98.0	98.8	98.6	98.8	98.9

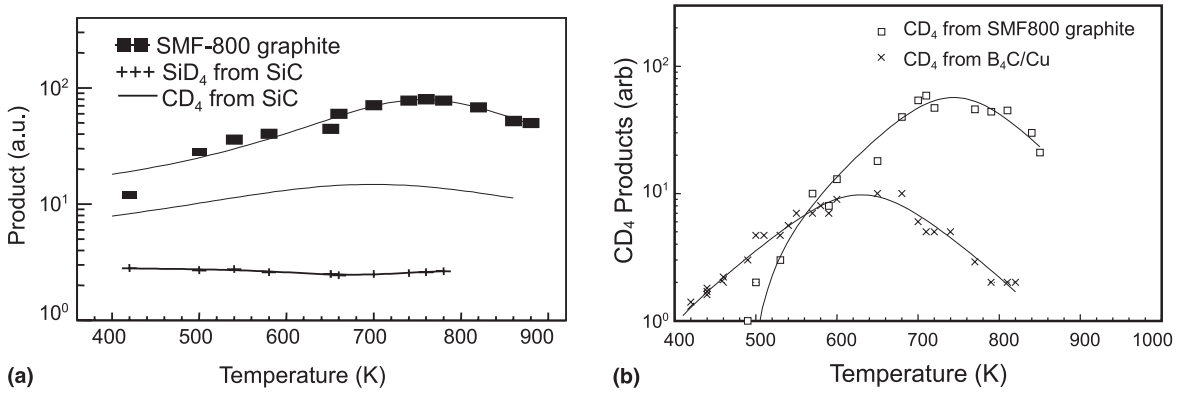

Fig. 1. (a) Temperature dependences of CD_4 and SiD_4 products under 3 keV, 4.6×10^{15} D^+/s cm^2 irradiation; (b) temperature dependences of CD_4 products under 3 keV, 4.6×10^{15} D^+/s cm^2 irradiation.

separately with a pore-making agent by ball milling. A green compact 40 mm in diameter × 3 mm thick was pressed in a steel die, then put in a graphite crucible embedded with Al_2O_3 powder and sintered at 1300°C for 1 h in a hydrogen atmosphere. A porous graded W skeleton was formed. Cu powder was then placed on the top of the W skeleton and sintered at 1300°C for 30 min; the melted Cu flowed into the pores of the W skeleton. Finally, a W plate was welded onto the other surface of the graded specimen by hot pressing, and a W/Cu FGM of five layers from 100% Cu on the top surface to 100% W on the bottom surface was formed. The bonding strength between the W layer and the transition layers was over 41 MPa. SEM observation revealed that a nearly continuous graded composition distribution was achieved.

3. Results and discussion

3.1. Chemical sputtering performance

The chemical sputtering performance of B_4C/Cu and SiC/C FGM was conducted in an LAS-2000 apparatus. The chemical sputtering yield was measured under conditions of irradiation by 3 keV D^+ ions at a flux of 4.6×10^{15} D^+/s cm^2. The chemical sputtering yield of SiC and B_4C/Cu FGM was ~20% that of SMF-800 graphite. As shown in Fig. 1, the peak value of CD_4 yield of B_4C/Cu FGM, which is reached at 660 K, is about 17% of that of SMF-800 graphite. The SiD_4 and CD_4 products at 500 K of SiC are 2.8 and 10 (arbitrary units), respectively. The total $SiD_4 + CD_4$ product of SiC at 500 K is 47% that of graphite SMF-800, while at 700 K it is 22% that of graphite. In comparison with SMF-800 graphite, SiC shows lower chemical sputtering yield.

3.2. Thermal desorption performance of B_4C/Cu coating FGM

The CH_4 thermal desorption spectra of specimens C1 and C3 are shown in Fig. 2. The main desorption peaks are at ~570 and ~770 K. Compared with high-purity SMF-800 graphite and boron-containing graphite, the characteristic desorption peak (770 K) is shifted to a lower temperature. The total CH_4 yield is 30–50% lower than that of SMF-800 graphite. This result is consistent with those reported in previous studies [14–16]. It is suggested that the desorption peak at 570 K corresponds to the free diffusion of CH_4 in internal micro-channels due to the porosity of the specimen.

3.3. Thermal shock experiment on B_4C/Cu FGM

Preliminary thermal shock experiments were conducted on specimens C1, C2, C3 and C4 in a electron-beam apparatus with the following experimental

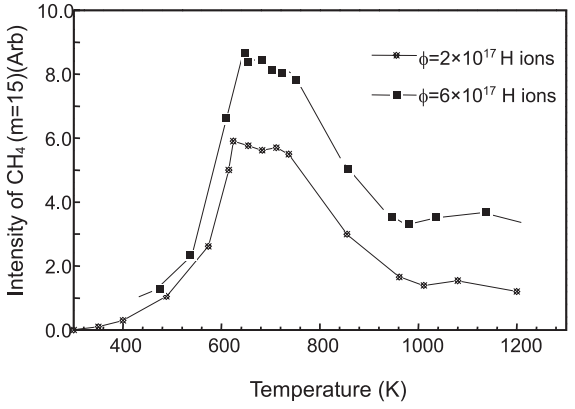

Fig. 2. Spectra of CH_4 thermal desorption of specimens C1 and C3.

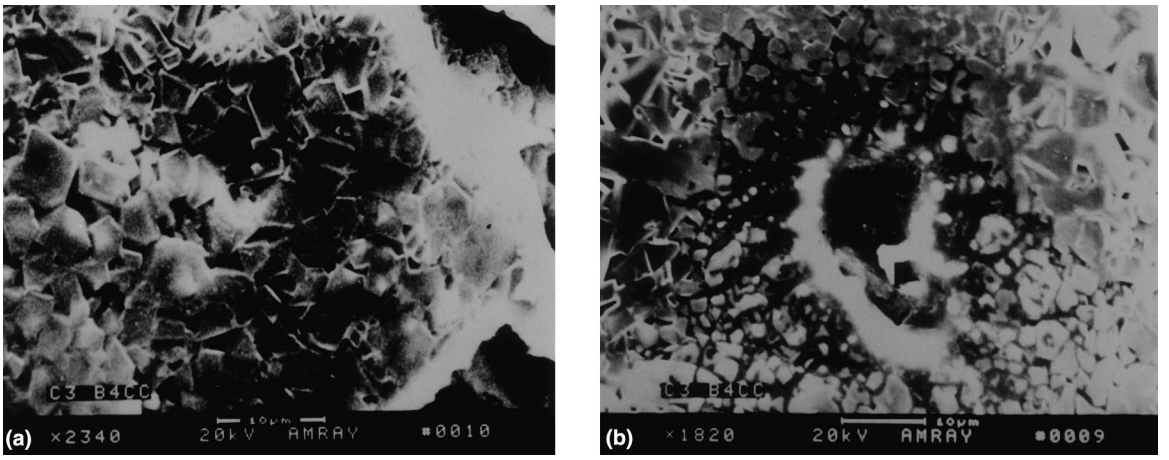

Fig. 3. SEM micrographs of specimen C3 after thermal shock experiment (a) near the beam spot and (b) in the center of the beam spot.

parameters:

Number of pulses	30
Pulse width	2 ms
Electron current	400 mA
Energy of electron beam	5000 eV

Cracks occurred in specimens C1 and C2, while basically no damage occurred in specimens C3 and C4 after 30 pulses. This result demonstrates that B_4C/Cu FGM has better thermal shock performance than B_4C/Cu non-FGM. On the basis of the result of preliminary tests, 250 pulses of thermal shock were applied to specimens C3 and C4. The coating layer at the periphery of the beam spot cracked in specimen C3, while cracking occurred within the beam spot in specimen C4. This difference might be attributed to a change of location of the beam spot during the experiment. Besides cracks, thermal shock changed the microstructure of specimens of C3 and C4. After thermal shock, the morphology of B_4C grains near the beam spot was clearly seen and different from that in the center of the beam spot, where some grains melted and formed a long chain, as shown in Fig. 3.

Thermal shock experiments were conducted in the electron-beam apparatus on a coating FGM specimen with $P = 1$ and coating thickness 300–400 μm with a 6.4 MW/m^2 and 1000 ms pulse. It is shown that no cracks and only small damages appeared after 1000 cycles.

3.4. Physical sputtering damage after plasma irradiation in HL-1M apparatus

The physical sputtering damage to the surface of specimen C1 (which should be the same for C3) was lower than that of the SMF-800 graphite specimen. No distinct change in crystal structure was found in the XRD pattern of specimen C1, while a small increase in peak width in the XRD patterns of the SMF-800 graphite specimen was observed, indicating a slight change in crystal structure and an increase of crystal lattice defects.

After plasma irradiation, evidence of plasma sputtering damage was noticed in SMF-800 graphite, while less evidence of plasma sputtering damage appeared in specimen C1.

4. Conclusions

Three different processing technologies have been used to produce SiC/C FGM, B_4C/Cu FGM and W/Cu FGM. Evaluation of structures and physical properties and primary investigation of some plasma-relevant performances show that these three kinds of FGM have promise as plasma-facing materials in fusion reactors.

Acknowledgements

This work is supported by the China National Committee of High Technology New Materials. The grant number is 863-715-011-0230.

References

[1] J.P. Qian, J. Roth, J.R. Song, F. Zhong, L. Yang, G.T. Zhai, J. Nucl. Mater. 258–263 (1998) 706.
[2] J. Linke, R. Duwe, A. Gervash, R.H. Qian, M. Roedig, A. Schuster, J. Nucl. Mater. 258–263 (1998) 634.
[3] M. Bolden, J. Roth, C.H. Wu, J. Nucl. Mater. 258–263 (1998) 740.

[4] V. Philipps, A. Pospieszczyk, U. Samm, J. Winter, H.G. Esser, M. Erdweg, L. Koenen, J. Linke, B. Schweer, J.V. Seggern, B. Unterberg, E. Vietzke, J. Nucl. Mater. 196–198 (1992) 1106.
[5] E. Vietzke, V. Philipps, K. Flaskamp, J. Nucl. Mater. 196–198 (1992) 1112.
[6] E.V. Dyomina, P. Fenici, U.P. Kolotov, M. Zucchetti, J. Nucl. Mater. 258–263 (1998) 1784.
[7] M. Onoiuka, S. Tsujimura, M. Toyoda, M. Inone, T. Abeand, Y. Muranami, Fus. Technol. 29 (1996) 73.
[8] M. Lipa, E. Gauthier, in: K. Herschbach, W. Maurer, J.E. Vetter (Eds.), Fusion Technology, 1994, Elsevier Science, Amsterdam, 1995, p. 455.
[9] H. Bolt, M. Aaraki, Fus. Technol. 29 (1996).
[10] I. Smid, M. Akiba, G. Vieider, C. Ploechl, J. Nucl. Mater. 258–263 (1998) 160.
[11] T. Hirai, in: Richard J. Brook (Ed.), Materials Science and Technology: A Comprehensive Treatment, Vol. 17B, Processing of Ceramics, Part 2, Weinheim Verlagsgesellschaft, Weinheim, 1996.
[12] C.C. Ge, Z.X. Wang, W. Cao, Int. J. SHS 7 (1998) 309.
[13] Z.X. Wang, Z.C. Mu, C.C. Ge, Int. J. SHS 6 (1997) 405.
[14] M. Yamawaki, K. Yamatuchi, Mater. Sci. Eng. 1140 (1991) 809.
[15] K. Yamatuchi, R. Ohmori, Fus. Eng. Des. 16 (1991) 387.
[16] V.Kh. Alimov, R. Schworer, J. Nucl. Mater. 187 (1992) 191.